Bone Marrow Mesenchymal Stem Cells Derived From Juvenile Macaques Reversed Ovarian Aging in Elderly Macaques

Chuan Tian
Guizhou Medical University
Jie He
Kunming General Hospital of the People's Liberation Army: People's Liberation Army Joint Logistic Support Force 920th Hospital
Yuanyuan An
Guizhou Medical University
Zailing Yang
Guizhou Medical University
Donghai Yan
Kunming General Hospital of the People's Liberation Army: People's Liberation Army Joint Logistic Support Force 920th Hospital
Hang Pan
Kunming General Hospital of the People's Liberation Army: People's Liberation Army Joint Logistic Support Force 920th Hospital
Guanke Lv
Kunming General Hospital of the People's Liberation Army: People's Liberation Army Joint Logistic Support Force 920th Hospital
Ye Li
Kunming General Hospital of the People's Liberation Army: People's Liberation Army Joint Logistic Support Force 920th Hospital
Yanying Wang
Kunming General Hospital of the People's Liberation Army: People's Liberation Army Joint Logistic Support Force 920th Hospital
Yukun Yang
Kunming General Hospital of the People's Liberation Army: People's Liberation Army Joint Logistic Support Force 920th Hospital
Gaohong Zhu
Kunming Medical College: Kunming Medical University
Zhixu He
Zunyi Medical College: Zunyi Medical University

Xiangqing Zhu
Kunming General Hospital of the People's Liberation Army: People's Liberation Army Joint Logistic Support Force 920th Hospital
xinghua Pan (xinghuapankm@163.com)
Kunming General Hospital of the People's Liberation Army: People's Liberation Army Joint Logistic Support Force 920th Hospital

---

Research Article

Keywords: Macaque, BMMSCs, Ovarian aging

Posted Date: April 26th, 2021

DOI: https://doi.org/10.21203/rs.3.rs-403877/v1

Version of Record: A version of this preprint was published at Stem Cell Research & Therapy on August 18th, 2021. See the published version at https://doi.org/10.1186/s13287-021-02486-4.

Abstract

Background

Female sex hormone secretion and reproductive ability decrease with ageing. Bone marrow mesenchymal stem cells (BMMSCs) have been postulated to play a key role in treating ovarian senescence; however, the curative effect and mechanism are not clear.

Methods

We used the macaque ovarian senescence model and observed the structural and functional effects of juvenile BMMSCs in the treatment of ageing macaque ovaries. Moreover, to elucidate the molecular regulatory mechanism by which BMMSCs reverse ovarian senescence, RNA sequencing (RNA-seq) of the ovaries was used to identify key genes and signalling pathways associated with transcriptome profile changes.

Results

(1) The Rhesus monkey ovarian aging models were an average of 24 years old and had the following sex hormone levels: 0.28 ± 0.11 mIU/mL hFSH, 0.017 ± 0.009 mIU/mL hLH, 0.24 ± 0.042 ng/mL Testo, 51.86 ± 18.37 pg/mL ESTRDL, 0.13 ± 0.012 ng/mL Prog, 0.013 ± 0.012 hCG, and 11.96 ± 2.96 pmol/l AMH. The ovarian organ index was 0.057 ± 0.021, and the HE staining results showed almost no follicular structure, with only local atresia follicles observed. For young rhesus monkeys, the average age was 7 years old, and sex hormone levels were as follows: 0.043 ± 0.03 mIU/mL hFSH, 0.007 ± 0.009 mIU/mL hLH, 0.57 ± 0.15 ng/mL Testo, 123.2 ± 26.26 pg/mL ESTRDL, 0.28 ± 0.014 ng/mL Prog, 0.05 ± 0.012 hCG and 11.96 ± 2.96 pmol/l AMH. The ovarian organ index was 0.011 ± 0.005, and the HE staining results showed all levels of follicles, suggesting that senile ovaries occur in old macaques. (2) P4 generation BMMSCs presented a typical cell morphology, staining positive for Oil Red O, Alizarin Red, and Alcian Blue. The positive rates of CD29, CD34, CD90, and CD105 on the cell surface were 98, 0.98, 98.8, and 99.8%, respectively, in line with mesenchymal stem cell standards. (3) The PET-CT results showed that the ovarian volume in the elderly treatment group increased, the lesions decreased, and the metabolism was vigorous. (4) The level of sex hormone secretion generally recovered to the level of the follicular phase for the 3rd, 6th and 8th months after the treatment of BMMSCs. (5) The HE results showed that all levels of follicles were observed in the young control group, and the medulla and stroma were neatly arranged, whereas primitive, primary, secondary, and atretic follicles were observed in the elderly treatment group. In addition, the medulla and stroma had obvious boundaries with a small amount of calcium nodules in the young control group. while those in the elderly control group had essentially no follicular structure, with only atretic follicles were seen locally that were filled with connective tissue. Masson staining results showed that the proportion of collagen fibres was 10.61 ± 1.83% in the young control group, 56.79 ± 3.58% in the elderly control group, and 23.71 ± 2.4% in the elderly treatment group. TUNEL staining results

showed that cell apoptosis was 1.07 ± 0.04%, in the young control group was, 25.93 + 2.49% in the old control group, and 6.98 + 1.35% in the old treatment group. The immunohistochemistry results showed 114 ± 17, 73 ± 6, and 118 ± 18 blood vessels in the young control group, the elderly control group, and the elderly treatment group, respectively. Immunofluorescence staining showed a lack of expression of enhanced green fluorescence protein (E-GFP) in BMMSCs without from the old control group, while green fluorescence was observed in the old treatment group. (6) After the treatment of BMMSCs, 1258 genes were identified as being differentially expressed. The 3D-PCA trace showed that the ovaries of the macaques in the elderly treatment group shifted to that observed in the young group. The genes that were upregulated with age were downregulated after the stem cell treatment. Genes that are downregulated with age were upregulated after stem cell therapy, and the top 20 PPI network genes were enriched for the progesterone-mediated maturation of follicles, oocytes, and cell cycle categories.

Conclusions

BMMSCs derived from juvenile macaques can reverse ovarian aging in elderly macaques

Introduction

As females age, both fertility and the endocrine function of the ovaries naturally decline due to waning follicle numbers as well as ageing-related cellular dysfunction[1][2]. Currently, ovarian failure and endocrine disruption are not cured. Societal changes and the increasing desire to preserve fertility have led to various treatment methods, including sex hormone replacement, cytokines and traditional Chinese medicine (TCM) treatments, to treat ovarian ageing, which leads to decreased fertility and endocrine secretion. However, the long-term use of hormone replacement therapy may cause breast cancer, thrombosis and other diseases[3]. Cytokine therapy has not yet led to a large-scale cytokine industry, and this treatment is expensive, which is not conducive to widespread development[4]. TCM treatment can partially improve ovarian function, but the drug composition has not been fully resolved, and there are many uncertain factors[5]. Although assisted reproductive technologies (ARTs) and the "freeze-all" strategy of cryopreserving all oocytes or good-quality embryos have increased the range of options[6], the overall success rate is still very low for older women. Therefore, it is necessary to seek new and effective treatment methods.

Ageing ovaries mainly manifest as atrophy of tissue structure, functional degeneration, insufficient self-renewal ability of reproductive helper cells, and decreased secretion of sex hormones. Bone marrow mesenchymal stem cells (BMMSCs) have multidirectional differentiation potential, a strong self-renewal capacity and biological characteristics of exosomes secreted with various cytokines[7], and they may become a new method to delay or reverse ovarian ageing[8]. Many clinical and basic studies have shown the effectiveness of mesenchymal stem cells (MSCs) in the treatment of ovarian ageing, and they have been demonstrated to be a more effective cell type to improve ovarian function[9]. Human amniotic fluid MSCs (hAFMSCs) can restore ovarian physiological ageing (OPA) function[10]. Human placental MSCs

(hPMSCs) can inhibit oxidative stress and apoptosis, thereby improving ovarian function[11]. Exosomes secreted by human umbilical cord MSCs (hUC-MSCs) have a stimulatory effect on primordial follicles and accelerate follicular development[12]. These studies are sufficient to show that MSCs can regulate the secretion of female sex hormones and improve ovarian structure.

However, research on animal models for BMMSC treatment of ageing and other diseases focuses on small and medium-sized animals, there are few studies on primates, and systematic and standardized studies are also lacking. Therefore, we used the macaque ovarian senescence model as the research object, observed the structural and functional effects of juvenile macaque BMMSCs in the treatment of macaque ageing ovaries, explored the molecular regulatory mechanism by which BMMSCs reverse macaque ovarian ageing, and provided BMMSCs to treat ovarian ageing as a reference technical solution and theoretical basis.

Materials And Methods

Materials

Macaques, bone marrow mesenchymal stem cells and granule cell sources

Laboratory animals were provided by the Kunming Institute of Zoology, Chinese Academy of Sciences, and the experiments were performed at the Cell Biological Therapy Center of the 920th Hospital of the Chinese People's Liberation Army. Five healthy young female macaques, ten healthy elderly female macaques, and all macaques were fed at the Kunming Institute of Zoology, Chinese Academy of Sciences, and the environment was clean and dry and met the animal feeding standards. The BMMSCs of juvenile male rhesus monkeys were provided by our laboratory.

Methods

Evaluation of ovarian ageing models in elderly macaques

(1) According to the age, back and facial features of the macaques, 10 healthy elderly female macaques were screened, with an average age of 24 years and a weight of 4-8 kg; 5 healthy young female macaques, with an average age of 7 years and a weight of 4.5-8 kg. (2) Young and old rhesus monkeys were anaesthetized with 3% sodium pentobarbital (1 kg/mL) for 15 minutes, and the vacuum blood sampling method was used in stock. Five millilitres of whole blood was intravenously drawn, divided into a heparin tube, and allowed to stand for 2 hours. After coagulation of whole blood, centrifuge at 1000 rpm for 5 min, transfer the supernatant to 1.5 mL EP tubes, centrifuge at 3000 rpm for 3 min, aspirate 0.5 mL of supernatant into Unicel DXI800 Access Immunoassay System, and detect levels of AMH, human follicle-stimulating hormone (hFSH), hLH, hCG, progesterone, testosterone and oestradiol (E2). (3) Expose the abdominal cavity, find the position of the ovary, take the ovary out with the vagina and fallopian tube, rinse once with sterile normal saline, and remove the ovary with tweezers and surgical scissors. The blood was wiped off, weighed (g) with an electronic balance and photographed, and the ovarian organ

index of the old and young rhesus monkeys was counted. After the ovary was separated, one ovary was cut into 2 pieces in the horizontal and vertical directions, approximately 1 mm3 in size, and fixed in 4% paraformaldehyde solution for 24 h. The ovarian tissue was dehydrated, embedded in paraffin and sectioned, with a thickness of approximately 4 μm, and used for HE staining to observe the structure.

Identification of bone marrow mesenchymal stem cells

(1) Inject 3% sodium pentobarbital at 1 mL/kg intravenously into young rhesus monkeys. Bone marrow puncture was performed on the posterior upper meridian of the femur. 5 mL of bone marrow was drawn into a 20 mL syringe containing 5 mL of heparin sodium saline (100 U/mL), then transferred to a 50 mL centrifuge tube, and 40 mL 10% ammonium chloride was added Mix thoroughly, centrifuge at 1200 rpm for 5 min, discard the supernatant, add sterile saline to resuspend the cells, centrifuge at 1000 rpm for 5 min, repeat twice, collect the cell pellet in a sterile 15 mL centrifuge tube. (2) In a sterile ultraclean workbench, add 6 mL of DMEM/F12 medium containing 10% foetal bovine serum to a sterile 15 mL centrifuge tube, resuspend and mix slowly, and inoculate 3 mL to 15 mL containing 10% Place 2 bottles in T175 cell culture flasks of DMEM/F12 medium with foetal bovine serum, then place them in a cell culture incubator with 5% CO2, 37°C, and 100% saturated humidity. Observe whether there is any abnormality every other day, and continue culturing for 5 days. (3) Slowly aspirate the supernatant with a 10 mL pipette, then add 10 mL sterile saline to wash twice, then add 18 mL DMEM/F12 medium containing 10% foetal bovine serum, and place. Whether there was any abnormality every other day was observed, and the solution was changed every 2 days. (4) When the confluency of the cells reached 75%, discard the supernatant, add 10 mL of sterile saline to wash twice, add 3 mL containing 0.25% EDTA trypsin for digestion at 37°C for 3 min, and then add 6 mL containing Stop the digestion in DMEM/F12 medium with 10% foetal bovine serum, mix well, centrifuge at 1000 rpm for 3 min, discard the supernatant, add 6 mL of DMEM/F12 medium with 10% foetal bovine serum, resuspend, mix, and inoculate In the new T175 cell culture flask, culture in a cell incubator. (5) When the degree of cell fusion reached 80%-90%, passage expansion and culture, P4 generation BMMSCs were used for flow cytometric analysis of the proportion of BMMSC surface antigens CD29, CD34, CD90, CD105, adipogenic, osteogenic and chondrogenic induction and differentiation experiments based on previously published methods from our research group[13-16].

Macaques grouping and BMMSC transplantation treatment

(1) According to the advice of breeding experts from the Kunming Institute of Zoology, Chinese Academy of Sciences, 10 elderly macaques were randomly divided into groups, namely, 4 in the elderly model group (n=4), 6 in the elderly treatment group (n=6), and 5 in the young control group. (n=5). (2) When the P4 BMMSCs grew to approximately 90% in T175 cm^2, the supernatant was discarded, 15 mL of normal saline was added to wash the cells three times, the normal saline was discarded, and 3 mL of 0.25% EDTA trypsin was added for 3 min. The reaction was stopped by adding 6 mL of basic culture DMEM and centrifuged at 2000 r/min for 5 min. The supernatant was aspirated, 3 mL of physiological saline was added to resuspend the solution, and 10 μl was used to count the cells. The cell concentration was

adjusted to 2×10^6 cells/mL, and the mixture was transferred to a 50 mL centrifuge tube for use. (3) Macaques in the elderly treatment group were injected into the femoral vein at a dose of 10^7 cells/kg once a day every other day three consecutive times. The young control group and the elderly model group were infused with the same volume of saline at the same time.

PET-CT observation of ovarian structure and function

Before the experiment, the macaques were fasted for 6 h. After pentobarbital sodium was used to anaesthetize the macaques, they were injected intravenously with ^{18}F-FDG at an injection volume of 3.70-4.44 MBq/kg. After resting at room temperature for 60 min, they were whole-body scanned with a GE Discovery^{TM} PETT/CT Elite. CT uses conventional whole-body spiral scanning with the following conditions: tube voltage 120 kV, tube current 240 mA, pitch 0.561, rotation speed 0.5 s/week, layer thickness 3.75 mm, spacing 512X512; PET has one bed every two minutes. After the image was collected, BestDicom software was used to analyse the different cross sections, and the SUVmax and CT values were counted.

Detection of sex hormone levels in peripheral blood

Five millilitres of peripheral blood was collected into a heparin tube after injecting the BMMSCs at 3, 6 and 8 months, and the blood was centrifuged at 1500 r/min for 5 min. The supernatant was transferred to a 1.5-mL EP tube and centrifuged at 3000 r/min for 3 min; 0.5 mL of the supernatant was added to the Unicel DXI800 Access Immunoassay System to detect the expression levels of AMH, hFSH, hLH, prolactin (PRL), progesterone, testosterone and E_2.

Macaque ovarian tissue collection

After 8 months of treatment with BMMSCs, the macaque was euthanized by anaesthesia with an excess of 3% sodium pentobarbital (1 kg/mL), exposed the abdominal cavity, found the position of the ovary, and removed the ovary with the vagina and fallopian tube, Rinse with sterile saline once, remove the ovaries with tweezers and surgical scissors, wipe the blood stains, weigh (g) on an electronic balance and take pictures. (2) After separating the ovary, one ovary was cut into 4 pieces in the horizontal and vertical directions, approximately 1 mm^3 in size, half of which were placed in a cryopreservation tube, added to 1.8 mL RNA protection solution, and stored in liquid nitrogen for RNA-seq. One ovary was fixed in 4% paraformaldehyde solution for 24 h, dehydrated, embedded in paraffin and sectioned at a thickness of approximately 4 μm for use in various subsequent histopathological tests.

H&E staining of ovarian tissue

The sections were put into xylene I for 20 min, xylene II for 20 min, absolute ethanol I for 5 min, absolute ethanol II for 5 min, and 75% alcohol for 5 min and washed 3 times with tap water. Then, put it into 5 mL of haematoxylin staining solution, dye for 3~5 minutes, wash 3 times with tap water, differentiate the differentiation solution for 5 minutes, wash 3 times with tap water, return the blue solution to blue for 5

minutes, and rinse slowly with running water 3 times. Then, the slices were placed into 85% and 95% gradient alcohols, dehydrated for 5 minutes each, and added to the eosin staining solution for 5 minutes. Then, the sections were put into absolute ethanol I for 5 min, absolute ethanol II for 5 min, absolute ethanol III for 5 min, xylene I for 5 min, and xylene II for 5 min for transparency, and the slides were sealed with neutral gum. Finally, microscopic examination, image acquisition and analysis were performed.

Masson staining of ovarian tissue

First, the sections were placed in xylene 2 times for 20 min, absolute ethanol 2 times for 5 min, and 75% alcohol for 5 min. Then, the slices were immersed in Masson A solution, soaked overnight, and washed with tap water 3 times the next day. After the slices were immersed for 1 min, they were washed with tap water 3 times, differentiated with 1% hydrochloric acid and alcohol, and washed with tap water 3 times. The slices were placed in Masson D solution for 6 min, rinsed with tap water 3 times, and then Masson E solution was used for 1 min. After slight draining, the slices were placed directly in Masson F solution and dyed for 20-30 s. Then, the sections were rinsed and differentiated with 1% glacial acetic acid, and two cylinders of absolute ethanol were dehydrated. Then, the slices were placed in the third container of absolute ethanol for 5 min, cleared with xylene for 5 min, and sealed with neutral gum. Finally, microscopic inspection, image acquisition and analysis were performed.

TUNEL staining of ovarian tissue

The frozen section was placed horizontally at 37°C for 15 min, 4% paraformaldehyde for 30 min, and PBS (pH 7.4) for 15 min. The sections were decolorized by shaking and washing on a decolorizing shaker 3 times for 5 min each. The proteinase K working solution was dropped in the circle to cover the tissue, and the section was incubated for 25 min in a 37°C incubator. Then, the slides were placed in PBS and washed with shaking on a decolorizing shaker 3 times for 5 min each time. The membrane rupture working solution was added to cover the tissues, and the samples were incubated at room temperature for 20 min. Furthermore, the slices were placed in PBS, shaken and washed 3 times for 5 min each time. Then, 1x Equilibration Buffer was added dropwise to cover the entire sample area to be tested, and the samples were incubated at room temperature for 10 min. The reaction solution was added: Recombinant TDT Enzyme, BrightRed Labelling Mix, 5x Equilibration Buffer and deionized water at a 1:5:10:34 ratio, and the solution was slowly dropped into the circle to cover the tissue. Subsequently, the slices were laid flat in a wet box and incubated for 2 h in a 37°C incubator. After fully aspirating the PBS, DAPI staining solution was added dropwise to the circle and incubated at room temperature in the dark for 10 min. The slices were placed in PBS, washed and shaken 3 times for 5 min each time. After the slices were slightly dried, the tablets were mounted with anti-fluorescence quenching. Finally, Microscopic examination.

Immunohistochemical staining to detect CD34 in ovarian tissue

The sections were put into xylene 2 times for 20 min, absolute ethanol 2 times for 5 min, 75% alcohol for 5 min, and washed with double distilled water 3 times. The tissue sections were placed in EDTA antigen retrieval solution, placed in a microwave oven for 8 min, stopped for 8 min, turned to medium and low

power for 7 min for antigen retrieval. The slides were washed in PBS 3 times for 5 min each time. BSA was added dropwise, and the samples were incubated for 30 min. CD34 antibody (1:3000) was added, incubated overnight and then washed 3 times in PBS for 5 min each time. The secondary antibody was added and incubated for 50 min at room temperature in the dark. An anti-fluorescence quenching mounter was added to the centre of the circle to mount the slide. DAPI dye solution was added dropwise to the circle and incubated for 10 min at room temperature in the dark. The sections were washed 3 times with PBS for 5 min each time. According to the proofreading counting method of Weidner *et al*, blood vessels were counted.

Immunofluorescence staining of ovarian tissue

The sections were placed in xylene 2 times for 15 min, absolute ethanol 2 times for 5 min, 85% alcohol for 5 min, 75% alcohol for 5 min, and then washed three times with distilled water. Then, draw a circle with a tissue brush around the position of the tissue section. DAPI staining solution was added dropwise to the circle and incubated at room temperature for 10 min in the dark. The slices were placed in PBS, shaken and washed 3 times for 5 min each time on a decolorizing shaker. After the slices were slightly dried, anti-fluorescence quenching and blocking tablets were added for mounting. Finally, the slices were observed under a fluorescence microscope and then scanned.

Transcriptome sequencing of ovarian tissue

The ovarian tissue was ground and lysed, after which total RNA was extracted and sequenced. The raw data were obtained by high-throughput sequencing, and reads were processed by removing adapters and quality control to obtain the clean reads. FastQC was used to analyse the quality of sequencing data and obtain relevant information such as sequencing quality distribution. Htseq-count was used to count the number of reads of some units in the genome. Differential expression analysis was performed with DESeq2, which performs cluster analysis of differentially expressed genes. The GO and pathway annotations of the differentially expressed genes obtained were analysed, and Fisher’s exact test was used to calculate the significance level (P-value) of each GO term and pathway to screen out those showing significant enrichment of differentially expressed genes and negatively related genes.

Statistical analysis

Statistical analyses were performed using SPSS 21.0. The data are expressed as the mean ± standard deviation. Significant differences between the means of three or more groups were analysed by one-way ANOVA

Results

Evaluation of research models on ovarian ageing in rhesus monkeys

Macaque research models of ovarian senescence were screened according to macaque age, sex hormone secretion, ovarian morphology, and HE staining. The results showed that the elderly macaques had an

average age of 24 years old, weighed 4 to 8 kg, and had a dim coat colour (Fig. 1 a and c). The sex hormone levels of these macaques are presented in Fig. 1 l: 0.28±0.11 mIU/mL hFSH, 0.017±0.009 mIU/mL hLH, 0.24±0.042 ng/mL Testo, 51.86±18.37 pg/mL ESTRDL, 0.13±0.012 ng/mL Prog, 0.013±0.012 hCG, and 11.96±2.96 pmol/l AMH. The ovarian atrophy (Fig. 1 f), ovarian organ index (0.011±0.005; Fig. 1 k), and HE staining results showed essentially no follicular structure, with only atresia follicles locally observed that were filled with fat and connective tissue (Fig. 1 i and j). The young macaques had an average age of 7 years old, weighed 4 to 8 kg, and had a bright coat colour (Fig. 1 b and d). The sex hormone levels of these macaques are presented in Fig. 1 l: 0.043±0.03 mIU/mL hFSH, 0.007±0.009 mIU/mL hLH, 0.57±0.15 ng/mL Testo, 123.2±26.26 pg/mL ESTRDL, 0.28±0.014 ng/mL Prog, 0.05±0.012 hCG, and 11.96±2.96 pmol/l AMH. The ovarian dilatation (Fig. 1 e), ovarian organ index (0.057±0.021; Fig. 1 k), and HE staining results showed that all levels of follicles could be observed, with the medulla and interstitial boundaries easily observed and eatly arranged (Fig. 1g and h).

Identification of bone marrow mesenchymal stem cells

The growth state of BMMSCs was observed under a fluorescent inverted phase contrast microscope. The results showed that a small number of primary BMMSCs migrated out in a short spindle shape after 3-4 days, and a large number of suspended impurities were present in the supernatant (Fig. 2 a). The P4 generation bone BMMSC fibroblast-like cells grew densely arranged in a spiral shape, exhibited a long spindle shape and showed obvious directionality, typical cell morphology characteristics, uniform morphology, and a strong refractive index (Fig. 2 b). Subsequently, the P4 generation BMMSCs were labelled with and expressed enhanced green fluorescent protein (E-GFP) (Fig. 2c).

Ovarian volume increases, basal metabolism improves, and sex hormonesfrom menopause recover to the follicular phase after treatment with BMMSCs.

PET-CT was used to analyse the changes in ovarian volume, standardized uptake value (SUV) max and CT values at 0, 3 and 6 months (Fig. 3 b). Our results showed that the ovarian volume was 0.31±0.11 cm^3 at 0 months (control), 1.43±0.73 cm^3 at 3 months, and 1.12±0.18 cm^3 at 6 months (Fig. 3 c). The SUV was 0.8±0.08 at 0 months (control), 1.4±0.43 at 3 months, and 1.17±0.12 at 6 months (Fig. 3 c). The CT value was 35.33±4.11 at 0 months (control), 55±2.45 at 3 months, and 53±2.16 at 6 months (Fig. 3 c).

The major functions of ovaries are to govern the health of an individual female by regulating endocrine status and the production of mature oocytes[17]. Therefore, the sex hormone levels in peripheral blood were assessed to evaluate the effect of BMMSCs on ageing ovaries. Compared to macaques that were not injected with BMMSCs at 0 months, testosterone levels increased at 3, 6 and 8 months. Progesterone levels increased at 3 and 6 months, decreased at 8 months and remained at a higher level than that observed at 0 months. hFSH levels increased at 3 months, decreased at 6 months and then increased at 8 months, indicating that the changes were not stable (Fig. 3 a). PRL levels decreased at 3 and 6 months and increased at 8 months to a level higher than that observed at 0 months (Fig. 3 a). The secretion of hLH decreased at 3 months and remained at a low level at 6 and 8 months (Fig. 3 a). E2 levels increased

at 3 months and then decreased at 6 and 8 months to a level higher than that observed at 0 months (Fig. 3 a). AMH levels increased at 3 months and decreased at 6 months (Fig. 3 a).

Improved ovarian histopathological structure with regenerated follicles occurred after treatment with BMMSCs for 8 months

Folliculogenesis is a precise and orderly process of internal coordination and external regulation in women[17]. A decline in ovarian function characterized by a decrease in both the quantity and quality of primordial follicles occurs with ageing. A recent study showed that hUC-MSC-exos can recover decreased fertility with increased oocyte production and improved oocyte quality in female mice[18]. The ovarian histopathological structural changes reflected the therapeutic effect of BMMSCs. Interestingly, the morphology of ovaries were improved after treatment with BMMSCs (Fig. 4 a). First, H&E staining was performed to observe the ovarian tissue structure and follicles (Fig. 4 b). The results showed that primordial, primary, secondary (red arrow) and mature follicles (blue arrow) could be observed, and contextual interstitial communication was obvious in the young control group. There were no obvious follicle structures, large amounts of connective tissue (green arrow), brown-yellow pigment deposition (black arrows), or more collagen fibres in local areas in the elderly model group. A number of primordial follicles, primary follicles and secondary follicles (red arrow) were generated; atresia follicles were observed; follicular zona pellucida showed disintegration; oocytes were not clearly demarcated; the zona pellucida was collapsed; and oocytes were irregularly shaped in the elderly treatment group.

Fibrosis is a hallmark of ageing tissues, and the ovary is the first organ to show overt signs of ageing. Recent studies have demonstrated that ageing often leads to altered ovarian rchitecture and function, including increased fibrosis in the ovarian stroma. hUMSC transplantation has been shown to be an effective method to inhibit ovarian fibrosis and to repair ovarian function in POI rats[19, 20]. Second, Masson staining was performed to observe the degree of fibrosis (Fig. 4 c, blue represents collagen fibres, and red represents muscle fibres), we observed that the ratio of collagen fibres was 10.61±1.83%, in the young control group and 56.79±3.58% in the elderly model group, The deposition area was large, well arranged and disordered, with few muscle fibres located locally. In the elderly treatment group 23.71±2.4%, of collagen fibres were mostly deposited in the cortex layer, the deposition area was small, and the arrangement was loose (Fig. 4 c and e).

Follicular atresia is related to the apoptosis of granulosa cells, which are large in ovarian follicles[21]. A previous study showed that UC-MSCs can promote the apoptosis of SKOV3 cells by regulating the expression of Bcl-2 and Bax[22]. Third, TUNEL staining was performed to analyse the rate of ovarian tissue apoptotic cells, where cells stained red were apoptotic (Fig. 4 d). The results showed that the young control group apoptotic rate was 1.07±0.04%, the elderly model group apoptotic rate was 25.93±2.49%, and the elderly treatment group apoptotic rate was 6.98±1.35% (Fig. 4 g).

Previous studies have observed that MSC-exos can augment the density of FITC-dextran perfused blood vessels and increase the number of intraepidermal nerve fibres in a diabetic mouse model[23], and intravenous injection of preconditioned MSC-IFNγ improves microvascular dynamics[24]. Finally, we

performed modified immunohistochemical staining to observe the density of blood vessels in the ovarian tissue, where the CD34-positive granules represent a blood vessel (Fig. 4 e). The results showed that 114±17, 73±6 and 118±18 blood vessels were observed in the elderly treatment group, the elderly model group, and the young control group, respectively (Fig. 4 g).

From the observed endocrinology and ovarian histology changes, it can be seen that BMMSCs reverse ovarian ageing, and to assess if BMMSCs exhibit homing to ovaries, immunofluorescence staining was performed to track BMMSCs in the ovary. The results showed that there were 3 immunofluorescent granules in the treatment group, while immunofluorescence was not observed in the elderly model group (Fig. 4 f).

A total of 1258 genes were differentially expressed, and ageing-related genes partly returned to a young phenotype following BMMSC treatment, with the function correlated to oocyte meiosis with maturation.

After observing the effect of BMMSCs on ovarian ageing with respect to improving ovarian tissue structure, RNA-seq was performed on ovarian tissue to identify the key genes and signalling pathways. Cluster plots showed that there were 1258 differentially expressed genes associated with ovarian ageing (Fig. 5 a). PCA trajectory analysis showed that after treatment with BMMSCs, the ageing-related genes of the elderly treatment group reversed back to the expression state of the young group (Fig. 5 b). GO analysis revealed that in general, the differentially expressed genes were primarily enriched for the cell cycle, DNA replication and cell adhesion molecules (Fig. 5 c). Four hundred fifteen genes were upregulated with ageing and downregulated after treatment with BMMSCs and were enriched for the cell cycle, chromosome segregation and cell division (Fig. 5 d) Eight hundred forty-three genes were downregulated with ageing and upregulated after treated with BMMSCs and were enriched for NABA MATRISOME, cytokine-mediated signalling pathways and metal ion homeostasis (Fig. 5 e). CytoHubba analysis screened the top 20 genes (Fig. 5 f), and ClueGO analysis showed that they were primarily enriched in the cell cycle, oocyte meiosis, and progesterone-mediated oocyte maturation (Fig. 5 g).

Discussion

Ovarian aging weakens female reproductive, ovulation, secretion of sex hormones and other functions and affects the tissues and organs of the body and is a gradual, multi-factorial, and complex biological process caused by the combined effect of the decreased number and quality of follicles. MSC transplantation has been shown to be effective and safe as a new therapeutic method for ovarian ageing[25], and these cells have been proposed to restore the function and structure of injured ovarian tissues[26]. Interestingly, our results provide a comprehensive understanding of the regulation of BMMSC interactions with ovarian ageing.

In our present study, PET-CT was used to observe the structure and function of ovaries, the results of which showed that the ovarian volume in the elderly treatment group increased, the lesions decreased, and the metabolism was vigorous. Sex hormones are secreted by ovaries to carry out specific functions and can affect others organs, and the sex hormone levels were improved after treatment with BMMSCs,

similar to the sex hormone levels of women. Additionally, we observed that hFSH reached the luteal phase, while testosterone, progesterone, PRL, AMH, hLH and E2 levels recovered to the follicle phase. Some similar studies have also shown the effectiveness of BMMSCs in recovering sex hormone secretion. In hUC-MSCs transplanted into ageing mice, E2 and AMH increased, FSH decreased, ovarian structure improved, and the number of follicles increased[27]. The use of MSCs in treating OPA increased follicle numbers, improved hormone levels, promoted cell proliferation, and inhibited apoptosis[28]. In a study of human adipose-derived mesenchymal stem cell-derived exosomes (hADSC-Exos) transplanted into a POI mouse model, hADSC-Exos could improve the number of follicles and increase hormone levels to normal levels[29]. In a study of stem Leydig cell (SLC) transplantation for treating testosterone deficiency, the transplanted cells were regulated by the hypothalamic-pituitary-gonad (HPG) axis, which restored nerves required for testicular function by physiologically restoring changes in the serum levels of testosterone endocrine regulation[30]. Furthermore, another study demonstrated that adipose-derived stem cells (ADSCs) in different cell cycle stages can be adjusted by the oestrogen and progesterone concentrations[31], suggesting that after BMMSCs regulate the secretion of sex hormones, sex hormones may in turn regulate the biological function of MSCs.

A study of hAMSCs transplanted into the natural ovarian ageing (NOA) mouse model showed that hAMSCs has therapeutic activity on mouse ovarian function by improving the number of follicles over four stages[32]. In our present study, comparative analysis between the elderly treatment group and the elderly model group showed that BMMSCs can promote follicle regeneration. Interestingly, a previous study demonstrated the presence of adult oogonial stem cells (OSCs) in the adult axolotl salamander ovary and showed that ovarian injury induces OSC activation and functional regeneration of the ovaries. OSC activation resulted in rapid differentiation into new oocytes, and follicle cell proliferation promoted follicle maturation during ovarian regeneration[33]. These results indicate that transplanted BMMSCs home into ovaries or function via the paracrine pathway to regulate the ovarian microenvironment to activate OSCs to promote follicle regeneration and improve ovarian structure.

Ovaries typically become fibrotic with aging, which leads to ovarian structural and function injury. Therefore, one strategy to alleviate or reverse fibrotic ovaries is to provide therapy to aging ovaries. In our present study, ovarian tissue Masson staining results showed that the collagen fibre rate observed in the elderly treatment group was lower than that detected in the elderly model group but dramatically higher han that detected in the young control group. Additionally, some studies on MSCs showed similar effectiveness. A study on polycystic ovarian syndrome found that hUC-MSCs can effectively improve the pathology and function of ovarian tissue, downregulate proinflammatory factors and fibrosis-related genes in ovaries and affect the systemic inflammatory response[34]. In a study of human placenta-derived mesenchymal stem cell (hPMSC) transplantation to treat POF, hPMSCs were shown to participate in the recovery of ovarian function[35]. These results demonstrate that BMMSCs can reduce or reverse ovarian fibrosis by inhibiting the inflammatory response of ovarian tissue by secreting various immune and inflammation regulatory factors, but its regulation of ovarian tissue inflammation has not been shown to restore it to the level of young macaques.

The antiapoptotic and antioxidative effects of human ASC-CMs were previously confirmed in the ovaries and uterus of pregnant mice[36]. Interestingly, our TUNEL staining results showed that apoptosis in the elderly treatment group was lower than that of the elderly model group and higher than that detected in the young control group. Additionally, in a study of foetal liver MSCs (fMSCs) treated with cyclophosphamide (CTX) to induce follicle loss, fMSCs were shown to prevent follicle loss, restore sex hormone levels, inhibit the expression of apoptotic genes and improve antiapoptotic effects[37]. Another experiment involving the cocultivation of hADSC-Exos and POI hGCs found that hADSC-Exos can promote the proliferation of hGCs, inhibiting the rate of apoptosis[29]. These results suggest that BMMSCs can reduce the apoptosis of ageing ovarian cells to balance cell proliferation with apoptosis, although the recovery effect did not reach the level of young macaques.

Ovarian tissue transcriptome sequencing analysis from young to older macaque ovaries revealed that after treatment with BMMSCs, 1258 genes were differentially expressed, where 415 upregulated genes were mainly enriched in the cell cycle, chromosome segregation and cell division, and 843 downregulated genes were primarily enriched in NABA MATRISOME, cytokine-mediated signalling pathways and metal ion homeostasis. PCA trajectory analysis showed that ageing-related genes partly return to a young phenotype following BMMSC treatment. The top 20 PPI network analysis genes were primarily enriched in the cell cycle, oocyte meiosis, progesterone mediated oocyte maturation, histone serine kinase activity and protein threonine/histone/tyrosine serine kinase. These results suggested that BMMSCs regulate ovarian ageing through these hub genes and networks to recover the ovarian microenvironment and sex hormone levels to promote follicle regeneration and improve ovarian structure. Furthermore, in the treatment group, comprehensive ovarian histology improved, follicles appeared and transcriptome ageing-related genes returned to the levels observed in the young group, indicating that BMMSCs can reverse ovarian ageing.

Conclusions

i. The elderly macaques ovarian aging models revealed that ovarian organ index decreased, no follicular structure, only local atresia follicles were seen, hFSH and hLH were increased, Testo, ESTRDL, Prog, hCG and AMH were decreased .
ii. BMMSCs derived from juvenile macaques reversed ovarian aging in elderly macaques, which promotes follicle and blood vessel regeneration, improves ovarian structure, suppressed cell apoptosis, inhibits the degree of fibrosis.
iii. In the process of ovarian aging, genes that are upregulated with aging were downregulated after stem cell therapy, while genes that were downregulated with aging were upregulated after stem cell therapy and reversed to the expression observed for young ovaries, top 20 PPI network enriched in the cell cycle, oocyte meiosis, progesterone mediated oocyte maturation.

Abbreviations

Abbreviations	Full name
BMMSCs	Bone marrow mesenchymal stem cells
hFSH	human follicle-stimulating hormone
prog	progesterone
testo	testosterone
E2	oestradiol
^{18}F-FDG	β-2-[18 F]-Fluoro-2-deoxy-D-glucose
FBS	fetal bovine serum

Declarations

Ethical approval and consent to participate

Animal production licence number: SCXK (Dian) K2017-0003. The use of macaques was approved by the experimental animal ethics committee of the relying unit, and the approval number was Lengshen 2019-032 (Section)-01 with the animal licence number SYXK (Military) 2012-0039.

Consent for publication

Not applicable.

Availability of data and material

All data generated or analysed during this study are included in this published article.

Competing interests

The authors declare that they have no competing interests.

Funding

This work was supported by grants from the Yunnan Science and Technology Plan Project Major Science and Technology Project (2018ZF007)

Authors' contributions

Xiangqing Zhu and Xinghua Pan conceived and designed the study. Chuan Tian, Jie He, Zailing Yang, Hang Pan, Donghai Yan, Guanke Lv, Ye Li, Yukun Yang, Yanying Wang, Gaohong Zhu performed the experiments and collected the data. Chuan Tian wrote the manuscript. Yuanyuan An and Zhixu He assisted with the literature searches and revised the manuscript. All authors read and accepted the final version of the manuscript submitted for publication.

Acknowledgements

We thank everyone in our team assisting with the preparation of this manuscript.

References

1. Truman AM, Tilly JL, Woods DC. Ovarian regeneration: The potential for stem cell contribution in the postnatal ovary to sustained endocrine function. Mol Cell Endocrinol. 2017;445:74-84.
2. Ahmed TA, Ahmed SM, El-Gammal Z, Shouman S, Ahmed A, Mansour R, et al. Oocyte Aging: The Role of Cellular and Environmental Factors and Impact on Female Fertility. Adv Exp Med Biol. 2020;1247:109-23.
3. Connelly PJ, Marie FE, Perry C, Ewan J, Touyz RM, Currie G, et al. Gender-Affirming Hormone Therapy, Vascular Health and Cardiovascular Disease in Transgender Adults. Hypertension. 2019;74:1266-74.
4. Bouet PE, Boueilh T, de la Barca J, Boucret L, Blanchard S, Ferre-L'Hotellier V, et al. The cytokine profile of follicular fluid changes during ovarian ageing. J Gynecol Obstet Hum Reprod. 2020;49:101704.
5. Yang X, Wang W, Zhang Y, Wang J, Huang F. Moxibustion improves ovary function by suppressing apoptosis events and upregulating antioxidant defenses in natural aging ovary. Life Sci. 2019;229:166-72.
6. Bosch E, De Vos M, Humaidan P. The Future of Cryopreservation in Assisted Reproductive Technologies. Front Endocrinol (Lausanne). 2020;11:67.
7. Samakova A, Gazova A, Sabova N, Valaskova S, Jurikova M, Kyselovic J. The PI3k/Akt pathway is associated with angiogenesis, oxidative stress and survival of mesenchymal stem cells in pathophysiologic condition in ischemia. Physiol Res. 2019;68:S131-8.
8. Han Y, Li X, Zhang Y, Han Y, Chang F, Ding J. Mesenchymal Stem Cells for Regenerative Medicine. Cells-Basel. 2019;8.
9. Ding C, Li H, Wang Y, Wang F, Wu H, Chen R, et al. Different therapeutic effects of cells derived from human amniotic membrane on premature ovarian aging depend on distinct cellular biological characteristics. Stem Cell Res Ther. 2017;8:173.
10. Huang B, Ding C, Zou Q, Lu J, Wang W, Li H. Human Amniotic Fluid Mesenchymal Stem Cells Improve Ovarian Function During Physiological Aging by Resisting DNA Damage. Front Pharmacol. 2020;11:272.
11. Ding C, Zou Q, Wu Y, Lu J, Qian C, Li H, et al. EGF released from human placental mesenchymal stem cells improves premature ovarian insufficiency via NRF2/HO-1 activation. Aging (Albany NY). 2020;12:2992-3009.
12. Yang W, Zhang J, Xu B, He Y, Liu W, Li J, et al. HucMSC-Derived Exosomes Mitigate the Age-Related Retardation of Fertility in Female Mice. Mol Ther. 2020;28:1200-13.
13. Pan XH, Chen YH, Yang YK, Zhang XJ, Lin QK, Li ZA, et al. Relationship between senescence in macaques and bone marrow mesenchymal stem cells and the molecular mechanism. Aging (Albany

NY). 2019;11:590-614.

14. Pan XH, Huang X, Ruan GP, Pang RQ, Chen Q, Wang JX, et al. Umbilical cord mesenchymal stem cells are able to undergo differentiation into functional islet-like cells in type 2 diabetic tree shrews. Mol Cell Probes. 2017;34:1-12.
15. Pan XH, Lin QK, Yao X, Li ZA, Cai XM, Pang RQ, et al. Umbilical cord mesenchymal stem cells protect thymus structure and function in aged C57 mice by downregulating aging-related genes and upregulating autophagy- and anti-oxidative stress-related genes. Aging (Albany NY). 2020;12:16899-920.
16. Pan XH, Zhou J, Yao X, Shu J, Liu JF, Yang JY, et al. Transplantation of induced mesenchymal stem cells for treating chronic renal insufficiency. Plos One. 2017;12:e176273.
17. Zhang Y, Zhang H. [Research advances in regulating mechanisms of mammalian ovarian folliculogenesis]. Sheng Li Xue Bao. 2020;72:63-74.
18. Yang W, Zhang J, Xu B, He Y, Liu W, Li J, et al. HucMSC-Derived Exosomes Mitigate the Age-Related Retardation of Fertility in Female Mice. Mol Ther. 2020;28:1200-13.
19. Amargant F, Manuel SL, Tu Q, Parkes WS, Rivas F, Zhou LT, et al. Ovarian stiffness increases with age in the mammalian ovary and depends on collagen and hyaluronan matrices. Aging Cell. 2020:e13259.
20. Cui L, Bao H, Liu Z, Man X, Liu H, Hou Y, et al. hUMSCs regulate the differentiation of ovarian stromal cells via TGF-beta1/Smad3 signaling pathway to inhibit ovarian fibrosis to repair ovarian function in POI rats. Stem Cell Res Ther. 2020;11:386.
21. Zheng Y, Ma L, Liu N, Tang X, Guo S, Zhang B, et al. Autophagy and Apoptosis of Porcine Ovarian Granulosa Cells During Follicular Development. Animals (Basel). 2019;9.
22. Zhou L, Xiang J, Li L, Chen W, Xi X. [Effect of umbilical cord mesenchymal stem cells on proliferation and apoptosis of ovarian cancer cells]. Zhong Nan Da Xue Xue Bao Yi Xue Ban. 2019;44:1120-7.
23. Fan B, Li C, Szalad A, Wang L, Pan W, Zhang R, et al. Mesenchymal stromal cell-derived exosomes ameliorate peripheral neuropathy in a mouse model of diabetes. Diabetologia. 2020;63:431-43.
24. Baudry N, Starck J, Aussel C, Lund K, Aletti M, Duranteau J, et al. Effect of Preconditioned Mesenchymal Stromal Cells on Early Microvascular Disturbance in a Mouse Sepsis Model. Stem Cells Dev. 2019;28:1595-606.
25. Jiao W, Mi X, Qin Y, Zhao S. Stem Cell Transplantation Improves Ovarian Function through Paracrine Mechanisms. Curr Gene Ther. 2020.
26. Kim GA, Lee Y, Kim HJ, Oh HJ, Kang SK, Ra JC, et al. Intravenous human endothelial progenitor cell administration into aged mice enhances embryo development and oocyte quality by reducing inflammation, endoplasmic reticulum stress and apoptosis. J Vet Med Sci. 2018;80:1905-13.
27. Li J, Mao Q, He J, She H, Zhang Z, Yin C. Human umbilical cord mesenchymal stem cells improve the reserve function of perimenopausal ovary via a paracrine mechanism. Stem Cell Res Ther. 2017;8:55.

28. Huang B, Ding C, Zou Q, Lu J, Wang W, Li H. Human Amniotic Fluid Mesenchymal Stem Cells Improve Ovarian Function During Physiological Aging by Resisting DNA Damage. Front Pharmacol. 2020;11:272.
29. Huang B, Lu J, Ding C, Zou Q, Wang W, Li H. Exosomes derived from human adipose mesenchymal stem cells improve ovary function of premature ovarian insufficiency by targeting SMAD. Stem Cell Res Ther. 2018;9:216.
30. Zang ZJ, Wang J, Chen Z, Zhang Y, Gao Y, Su Z, et al. Transplantation of CD51(+) Stem Leydig Cells: A New Strategy for the Treatment of Testosterone Deficiency. Stem Cells. 2017;35:1222-32.
31. Li JN, Zhang Y, Wang YF, Chen JY. Effect of pregnancy on the proliferation of rat adipose-derived stem cells. Genet Mol Res. 2017;16.
32. Ding C, Zou Q, Wang F, Wu H, Chen R, Lv J, et al. Human amniotic mesenchymal stem cells improve ovarian function in natural aging through secreting hepatocyte growth factor and epidermal growth factor. Stem Cell Res Ther. 2018;9:55.
33. Erler P, Sweeney A, Monaghan JR. Regulation of Injury-Induced Ovarian Regeneration by Activation of Oogonial Stem Cells. Stem Cells. 2017;35:236-47.
34. Xie Q, Xiong X, Xiao N, He K, Chen M, Peng J, et al. Mesenchymal Stem Cells Alleviate DHEA-Induced Polycystic Ovary Syndrome (PCOS) by Inhibiting Inflammation in Mice. Stem Cells Int. 2019;2019:9782373.
35. Yin N, Wang Y, Lu X, Liu R, Zhang L, Zhao W, et al. hPMSC transplantation restoring ovarian function in premature ovarian failure mice is associated with change of Th17/Tc17 and Th17/Treg cell ratios through the PI3K/Akt signal pathway. Stem Cell Res Ther. 2018;9:37.
36. Ra K, Oh HJ, Kim GA, Kang SK, Ra JC, Lee BC. High Frequency of Intravenous Injection of Human Adipose Stem Cell Conditioned Medium Improved Embryo Development of Mice in Advanced Maternal Age through Antioxidant Effects. Animals (Basel). 2020;10.
37. Huang B, Qian C, Ding C, Meng Q, Zou Q, Li H. Fetal liver mesenchymal stem cells restore ovarian function in premature ovarian insufficiency by targeting MT1. Stem Cell Res Ther. 2019;10:362.

Figures

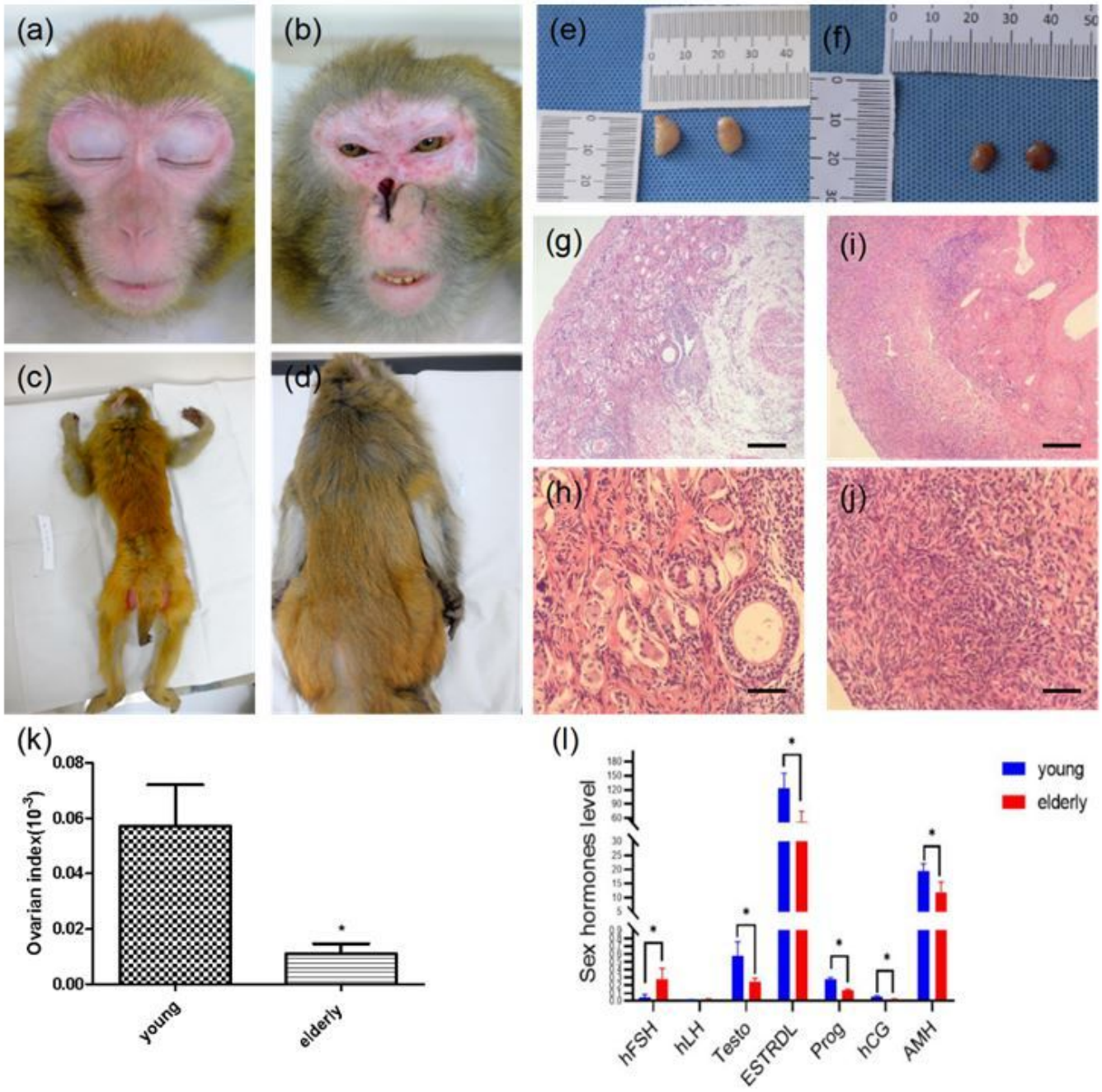

Figure 1

Evaluation of research models on ovarian ageing in elderly macaques. (a) Facial features of young macaques; (b) Facial features of old macaques; (c) Back features of young macaques; (d) Back features of old macaques; (e) Ovary morphology of young macaques; (f) Ovary morphology of old macaques; (g) HE staining of young macaques ovary (100×); (h) HE Staining of young macaques ovary (400×); (i) HE staining of old macaques ovary (100×); (j) HE staining of old macaques ovary (400×); (k) statistical analysis of ovarian organ index of young and old macaques; (l) statistical analysis of sex hormone secretion levels in young and old macaques.

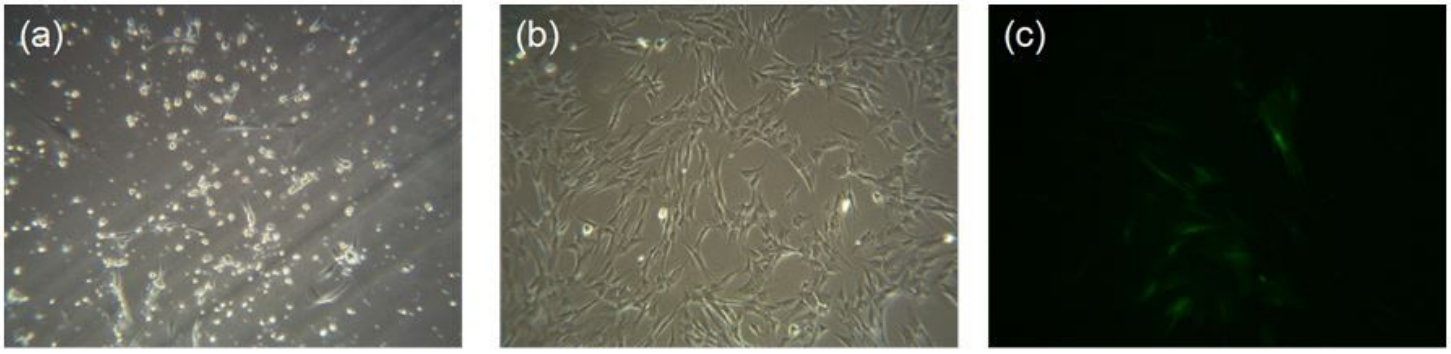

Figure 2

Morphology of bone marrow mesenchymal stem cells. (a) The primary generation of BMMSCs (100×); (b) The P4 generation of BMMSCs (100×); (c) The E-GFP-labelled BMMSCs (100×).

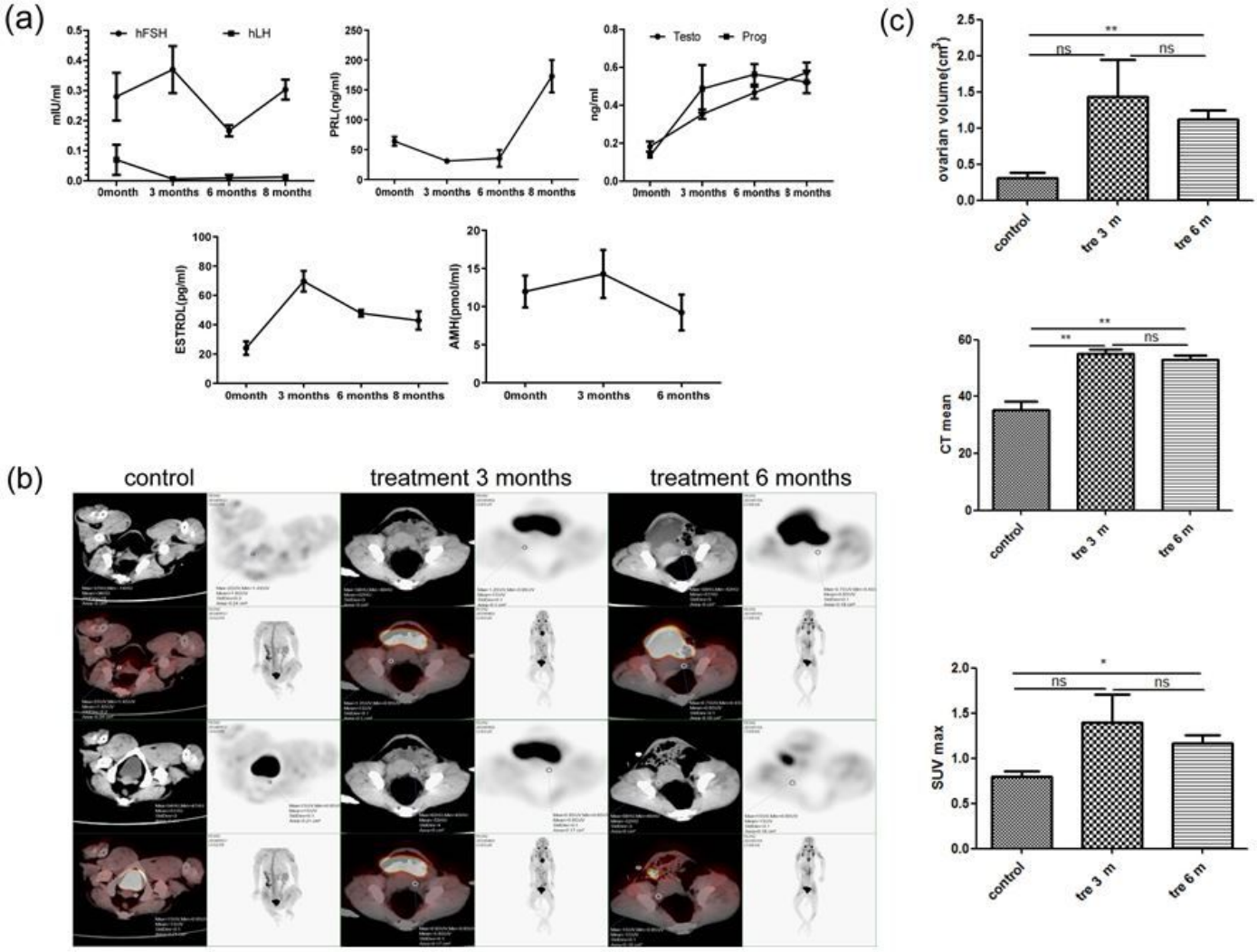

Figure 3

Changes in the levels of sex hormones ovarian volume, SUV max and CT value after treatment with BMMSCs. (a) Changes in hFSH, hLH, testosterone, progesterone, PRL, oestradiol and AMH expression after 3, 6 and 8 months. (b) PEC-CT was used to observe the changes in the ovarian SUV max and volume and CT value. Whiteness represents the ovarian structure, and redness represents metabolism. (c) Statistical analysis of the CT value, volume and SUV max.

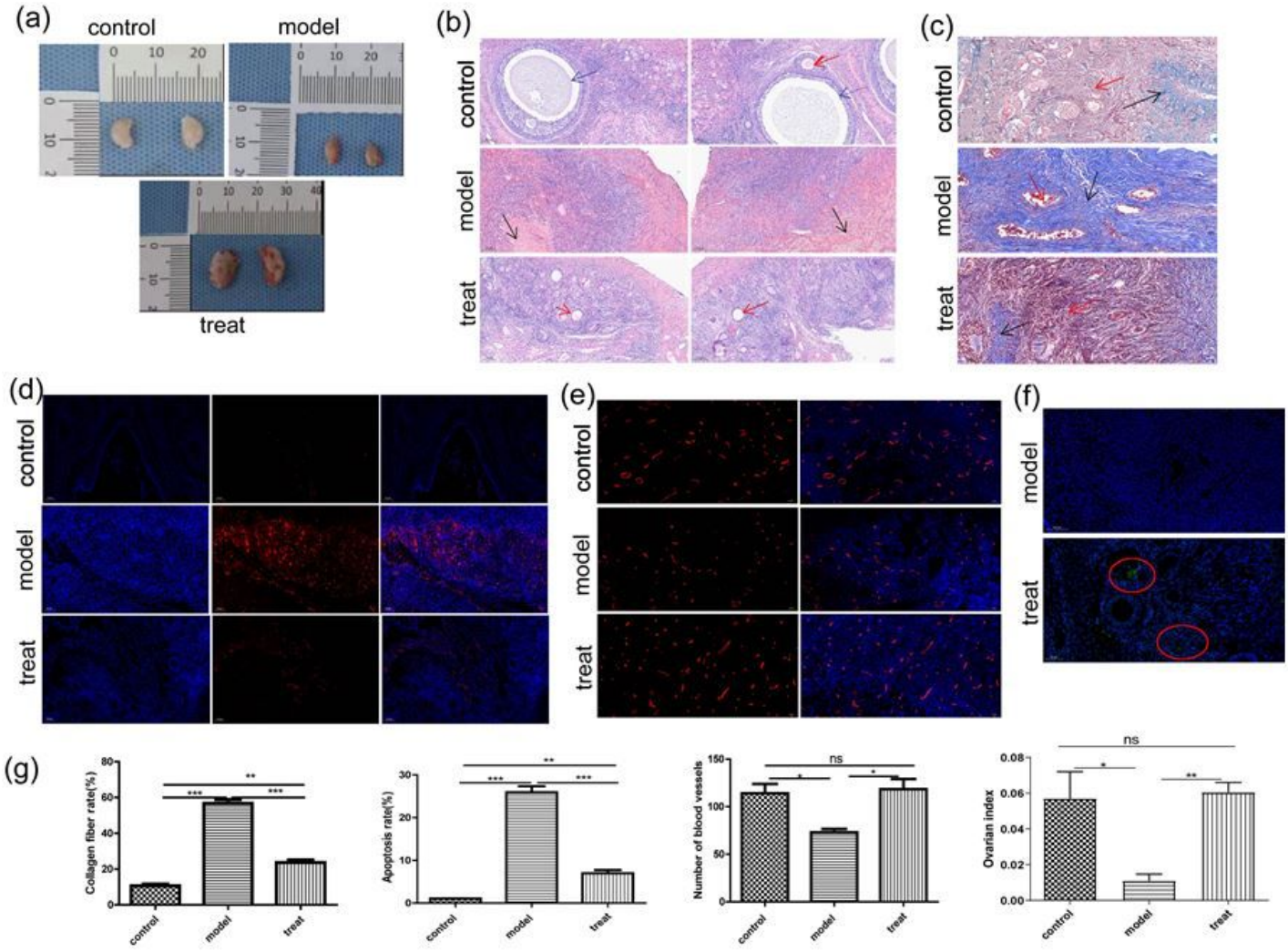

Figure 4

Ovarian histopathological observation after treatment with BMMSCs for 8 months. (a) The morphology of ovaries. (b) HE staining was performed to observe the ovarian tissue structure. (c) Masson staining was performed to observe the degree of fibrosis. (d) TUNEL staining was performed to analyse the ratio of apoptotic cells. (e) Immunohistochemical staining was performed to observe the density of blood vessels in the ovarian tissue. (f) Immunofluorescence staining was performed to track BMMSCs in the ovary. (g) Statistical analysis of the degree of fibrosis, the ratio of ovarian tissue apoptotic cells, the density of blood vessels and ovarian organ index (* $p < 0.05$, ** $p < 0.01$, and ***$p < 0.001$).

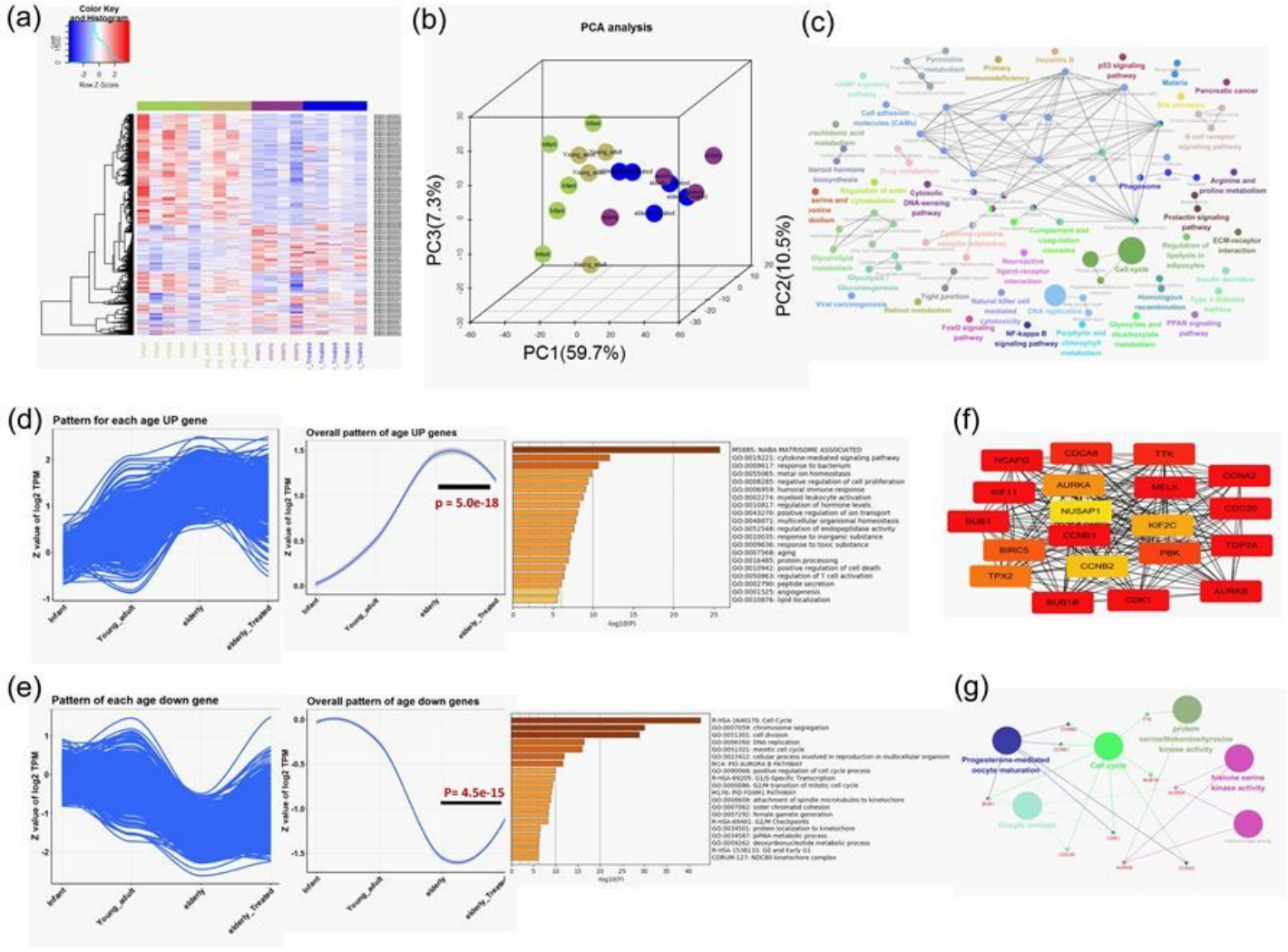

Figure 5

Transcriptome sequencing of ovarian tissues. (a) Cluster plot showing the 1258 differentially expressed genes. (b) PCA of ageing-related genes from the juvenile to GO-enriched elderly model group and the treatment group. (c) ClueGO analysis of 1258 differentially expressed genes with functional enrichment. (d) GO enrichment pattern for upregulated genes and 843 downregulated genes for the age and BMMSC treatment groups. (e) GO enrichment pattern for downregulated and 415 upregulated genes for the age and BMMSC treatment groups. (f) Cytohub screening of the top 20 genes with protein-protein interaction (PPI) network analysis. (g) Top 20 genes from the ClueGO function and pathway analyses.